Published in final edited form as:

Glia. 2018 May ; 66(5): 987–998. doi:10.1002/glia.23296.

MicroRNA-31 is Required for Astrocyte Specification

Gordon P. Meares[1,Δ], **Rajani Rajbhandari**[2,Δ], **Magda Gerigk**[3], **Chih-Liang Tien**[3], **Chenbei Chang**[3], **Samuel C. Fehling**[3], **Amber Rowse**[3], **Kayln C. Mulhern**[3], **Sindhu Nair**[2], **G. Kenneth Gray**[3], **Nicolas F. Berbari**[4], **Markus Bredel**[2], **Etty N. Benveniste**[3], and **Susan E. Nozell**[2,*]

[1]Departments of Microbiology, Immunology and Cell Biology, West Virginia University, Morgantown, West Virginia, 26506

[2]Radiation Oncology, University of Alabama at Birmingham, Birmingham, Alabama 35294

[3]Cell, Developmental and Integrative Biology, University of Alabama at Birmingham, Birmingham, Alabama 35294

[4]Biology, Indiana University-Purdue University Indianapolis, Indianapolis, Indiana, 46202

Abstract

Previously, we determined microRNA-31 (miR-31) is a non-coding tumor suppressive gene frequently deleted in glioblastoma (GBM); miR-31 suppresses tumor growth, in part, by limiting the activity of NF-κB. Herein, we expand our previous studies by characterizing the role of miR-31 during neural precursor cell (NPC) to astrocyte differentiation. We demonstrate that miR-31 expression and activity is suppressed in NPCs by stem cell factors such as Lin28, c-Myc, SOX2 and Oct4. However, during astrocytogenesis, miR-31 is induced by STAT3 and SMAD1/5/8, which mediate astrocyte differentiation. We determined miR-31 is required for terminal astrocyte differentiation, and that the loss of miR-31 impairs this process and/or prevents astrocyte maturation. We demonstrate that miR-31 promotes astrocyte development, in part, by reducing the levels of Lin28, a stem cell factor implicated in NPC renewal. These data suggest that miR-31 deletions may disrupt astrocyte development and/or homeostasis.

Keywords

microRNA-31; astrocytes; neural precursor cell; differentiation

[*]Corresponding author: Susan E. Nozell, Ph.D., Department of Radiation Oncology, 1700 6th Avenue South, Room 2220A, University of Alabama at Birmingham, Birmingham, Alabama 35294-0005, Phone: (205) 975-0521; Fax: (205) 975-4372; snozell@uab.edu.
[Δ]These authors contributed equally to this project.

Author Contributions

S.E.N., G.P.M., and E.N.B. conceived of the overall scientific premise, experimental design, interpreted the data and wrote the manuscript. G.P.M. and R.R. contributed equally to this work. S.E.N., R.R., and N.F.B. designed and performed the immunofluorescence (IF) studies. M.G., C.T. and C.C. designed and performed the *Xenopus laevis* studies. G.P.M and R.R. designed and executed all mouse studies. S.E.N. and G.K.G. performed GEO analyses. Except where noted elsewhere, R.R. executed all experiments from Figs. 4–9. S.E.N., S.N., and M.B. analyzed *in situ hybridization* presented in Fig. 3. S.C.F. performed the RNA immunoprecipitation studies. A.R. confirmed the identity of primary cells using flow cytometry. K.C.M. assisted with chromatin immunoprecipitation studies.

Disclosure of Potential Conflicts of Interest

The authors declare no competing financial interests.

Introduction

NPCs are the resident precursor cells within the brain. These cells have the ability to self-renew, are able to proliferate extensively and can differentiate into multiple neuroectodermal lineages (Dietrich et al. 2008). In the developing CNS, NPCs are found in the subgranular zone (SGZ) and subventricular zone (SVZ). NPCs differentiate in a step-wise process that involves patterning, specification, migration and terminal differentiation (Molofsky et al. 2012). Ultimately, these cells produce lineage-committed progenitors (glial-restricted, neuron-restricted, astrocyte and oligodendrocyte precursor cells) that give rise to terminally differentiated cells (astroctyes, neurons and oligodendrocytes) (Dietrich et al. 2008). In the adult brain, radial glial cells function as NPCs (Alvarez-Buylla et al. 2001; Chaker et al. 2016; Gallo and Deneen 2014; Maldonado-Soto et al. 2014; Namihira and Nakashima 2013; Noctor et al. 2001; Paul et al. 2017; Tome-Garcia et al. 2017). NPCs rely on general stem cell factors such as Lin28, Oct4 and SOX2, and tissue specific factors in order to self-renew (Aloia et al. 2013; Loh et al. 2006; Ronan et al. 2013; Tiwari et al. 2013). Lin28 is an RNA binding protein, while Oct4 and SOX2 are transcription factors (Shyh-Chang and Daley 2013). Collectively, these proteins promote the expression of genes required for NPC renewal, and inhibit the expression of genes that promote differentiation (Aloia et al. 2013; Loh et al. 2006). NPC to astrocyte differentiation is mediated by multiple factors/signaling molecules, including JAK/STAT3, BMP/Smads, NFIA and SOX9 (Dirks 2006; Gallo and Deneen 2014; Kim et al. 2011; Sieber et al. 2009). Together, Smads, STAT3, NFIA and SOX9 establish the transcriptional profile that mediates astrocytogenesis (Deneen et al. 2006; Fukuda et al. 2007; Gallo and Deneen 2014; Glasgow et al. 2014b; Kang et al. 2012).

MiRs are short, endogenous non-coding RNAs that bind to target mRNAs in order to prevent their translation or reduce their stability (Lujambio and Lowe 2012). MiR-31 is a non-coding tumor suppressor encoded by the *MIR31HG* gene located at 9p21.3, the most frequently deleted region in GBM (Rajbhandari et al. 2015). Previously, we demonstrated that one or both copies of *MIR31HG* are deleted in GBM, and that miR-31 restoration reduced tumor growth and improved survival in mouse models of GBM (Rajbhandari et al. 2015). Herein, we expand these findings and elaborate on the role of miR-31 during normal astrocyte development within the CNS. We find Lin28, Oct4 and SOX2 inhibit miR-31 expression and activity in NPCs. However, during astrocytogenesis, STAT3 and SMAD1/5/8 increased the levels of miR-31. Alone, exogenous miR-31 can partially promote astrocyte differentiation of NPCs; this is in part by targeting the stem cell factor Lin28. In the absence of miR-31, NPCs fail to fully differentiate into astrocytes. Finally, in astrocytes, we demonstrate that loss of miR-31 prevents astrocyte maturation and causes these cells to assume a more NPC-like phenotype. Collectively, these data indicate that miR-31 is critical for astrocyte development and/or commitment.

Materials and Methods

Reagents

IL-1β and TNF-α were from R & D Systems. The secondary peroxidase-conjugated antibodies and enhanced chemiluminescence reagents were purchased from Amersham (Arlington Heights, IL). Anti-KLF4, anti-Lin28, anti-Nestin, anti-Oct4 and anti-SOX2

antibodies were from Santa Cruz. Anti-Olig2 antibodies were purchased from R & D Systems. Anti-GFAP antibodies were from Pharmingen, and anti-Brn2 (POU3F2) and anti-GAPDH antibodies were from Abcam. Taqman qRT-PCR reagents were from Applied Biosystems (Beverly, MA). Sybr green qRT-PCR reagents were from Qiagen (Valencia, CA). All other primers were purchased from Integrated DNA Technologies (Iowa City, IA). MicroRNA-31 mimic, miR-31 AntagomiR and negative control (CT) miR were purchased from Ambion/Life Technologies (Austin, TX). MicroRNAs and shRNA molecules were transfected using Lipofectamine RNAiMax Transfection reagent (Life Technologies, Grand Island, NY). Control and Lin28 specific shRNA were purchased from Dharmacon.

Immunofluorescence

Where indicated, cells or cryosections were post-fixed in 4% PFA for 5 minutes at room temperature followed by three 5 minute washes in PBS followed by a Methanol treatment at −20°C for 15 minutes. Sections were then washed with PBS followed by permeabilization and blocking with 0.3% Triton X-100 in PBS with 2% donkey serum, 0.02% sodium azide and 10 mg/ml bovine serum albumin (BSA). Sections were then labeled with antibodies indicated, washed in PBS with 2% normal donkey serum, 0.02% sodium azide and 10 mg/ml BSA, and incubated in secondary antibody (1:1000, Alex Fluor-594, A-21203, Invitrogen, Carlsbad, CA). Nuclei were visualized by DAPI nuclear stain (Invitrogen, Carlsbad, CA). Sections were mounted onto glass slides and mounted using DABCO mounting media (10 mg of DABCO (D2522; Sigma-Aldrich, St. Louis, MO) in 1 mL of PBS and 9 mL of glycerol, and imaged using confocal microscopy (Koemeter-Cox et al. 2014).

Immunoblotting

Cells were lysed in RIPA buffer with protease inhibitors and protein concentration was determined using the BioRad dye-binding protein assay. Equivalent amounts of total protein were analyzed by SDS-PAGE with antibodies specified above, as previously described (McFarland et al. 2013; Rajbhandari et al. 2015).

Mice and Primary Cell Preparations

Normal primary murine NPCs were prepared as previously described (Meares et al. 2014). NPCs were plated in Neurobasal media with Amphotericin (1%), B27 Supplement minus vitamin A, Gentamycin (0.25%), L-glutamine (260 mM), EGF (10 ng/ml), and FGF (10 ng/ml) and cultured as neurospheres. NPC identity was confirmed by flow cytometry using antibodies specific for SOX2, Nestin and GFAP. Where appropriate, untreated and treated NPCs were grown as adherent cultures on laminin (1.2 μg/ml) and poly-D-lysine (62.5 μg/ml) coated plates. To induce differentiation, NPCs were cultured with 10% FBS or LIF (10 ng/ml) and/or BMP2 (10 ng/ml) for the times indicated. C57BL/6 mice were bred and housed in the animal facility at the University of Alabama in Birmingham under the care of the animal resources program. Primary murine astrocytes were prepared as previously described (Meares et al. 2013). Astrocytes were cultured in Dulbecco's modified Eagle's medium (DMEM) with 10% FBS, 16 mM HEPES, 1× nonessential amino acids, 2 mM l-glutamine, 100 units/ml penicillin, 100 μg/ml streptomycin, and 50 μg/ml gentamicin. Astrocytes were separated from microglia by shaking at 400 rpm for 2 h, and astrocyte

cultures contained >90% GFAP-positive cells, as determined by immunofluorescence microscopy.

Total RNA and microRNA Purification, and Real-Time qRT-PCR

Total RNA was isolated as previously described (McFarland et al. 2013; Rajbhandari et al. 2015). To assess mRNA expression levels, 1 μg of total RNA was reverse transcribed and analyzed by quantitative PCR. Reactions for each sample were performed in triplicate using a PCR protocol (95°C activation for 10 min followed by 40 cycles of 95°C for 15s and 60°C for 1 min) in an ABI StepOnePlus Detection System (Applied Biosystems). ΔΔCt values for genes were examined using Ct values generated by StepOnePlus software (Applied Biosystems). miRNA was purified using the miRvana miRNA isolation kit (Invitrogen, Grand Island, NY) according to manufacturer's protocol. For miRNA-31 analyses, 10 ng of miRNA was reverse transcribed and analyzed by quantitative PCR using a miR-31 specific first strand primer and probe/primer sets purchased from Applied Biosystem (Grand Island, NY).

Whole Mount In Situ Hybridization

The *X. laevis* embryos were collected at neurula stages and analyzed by whole mount *in situ* hybridization analyses for miR-31 and marker expression. *In situ* hybridization was performed as described (Harland 1991; Nie and Chang 2007), using the neural or the epidermal probes described previously (Tien et al. 2015). I*n situ* hybridization of horizontal sections of embryonic murine brains (E14.5) was performed using a modified method (Bonev and Papalopulu 2012).

ChIP Assays

ChIP assays were performed as previously described (Nozell et al. 2008; Rajbhandari et al. 2015; Tien et al. 2015). Immunoprecipitation was performed with 5 μg of the appropriate antibodies, and the immune complexes were absorbed with protein A beads (Upstate Cell Signaling Solutions, Charlottesville, VA) blocked with bovine serum albumin and salmon sperm DNA. Immunoprecipitated DNA was analyzed by qRT-PCR using Sybr Green reagents. Reactions for each sample were performed in triplicate using an ABI StepOnePlus Detection System (Applied Biosystems, Foster City, CA) and a PCR protocol comprising an initial 10 min incubation at 95°C followed by 40 cycles of 15 s at 95°C and 1 min at 60°C. The raw data were analyzed using StepOnePlus software (Applied Biosystems), and ΔΔCt values for each gene in each sample were determined.

Statistical Analysis

Student *t* tests were conducted for comparison of 2 values. Values represent the mean ± SD unless otherwise noted. $p < 0.05$ was considered statistically significant.

Ethics Statement

All animal experiments (C57BL/6, Harlan Laboratories) were performed with the approval of the University of Alabama at Birmingham Institutional Animal Care and Use Committee (APNs #120908862, #120309368 and #120809198).

Results

MicroRNA-31 Levels Increase During CNS Development

To understand the potential role of miR-31 during early CNS development, we first utilized *Xenopus laevis*; in this model, CNS development begins with neural plate in-folding followed by neural tube closure (Fig. 1A) (Schroeder 1970). As *Xenopus* embryos transition from early- to the mid-stages of neuralation, miR-31 levels become elevated (Fig. 1B). We used whole mount *in situ* hybridization (ISH) to determine which cells express miR-31; *XK70* (epidermal marker), *SOX2* (neural tube marker) and *Snail2* (neural crest marker) were also analyzed as cell-specific markers (Tien et al. 2015). At the mid neurula phase, the pattern of miR-31 expression appeared most similar to that of *SOX2* expression, but did not appear similar to the patterns of *XK70* or *Snail2* (Fig. 1C). Double ISH of *X. laevis* embryos confirmed miR-31 (green arrow) was co-expressed with *SOX2* (orange arrow) in the neural tube, but not with *Snail2* (white arrow; right), which marks the neural crest (Fig. 1D). These data indicate miR-31 may play an early role in neural but not epidermal or neural crest specification.

Next, we assessed the role of miR-31 in later stages of CNS development using mice. MiR-31 levels were analyzed from whole murine brain samples of mice aged embryonic (E) E15 to parental (P) P70 by qRT-PCR; we found that miR-31 levels increased from E15 to P70 (Fig. 1E). We also evaluated *Nestin*, *Lin28B*, *Oct4* and *GFAP* mRNA levels. Nestin marks NPCs, Lin28 and Oct4 are stem cell markers, and GFAP specifies astrocytes. At these same developmental stages, we found that the levels of *Nestin*, *Lin28B*, and *Oct4* were diminished (Fig. 1F), while the levels of GFAP were increased (Fig. 1G). Thus, the levels of miR-31 increase during astrocytogenesis (E15–P70) and correlate with elevated GFAP levels.

We also evaluated miR-31 expression in the developing mouse brain at E14.5 using *ISH*; samples were counterstained with DAPI to mark cell nuclei (Fig. 2A, blue; i, iii, v). This developmental stage (E14.5) marks the neurogenic-to-gliogenic switch (Liu et al. 2002; Martynoga et al. 2012); miR-31 was diffusively expressed throughout the brain (Fig. 2A, green). MiR-31 levels were notable in the Infudibulum (IF; 2A, i and ii), particularly in the ventricular zone (VZ) surrounding the Aqueduct of Sylvius (AQ) (Fig. 2A, i and ii) (Schambra et al. 1991). The VZ is formed by multipotent radial glial and/or neural stem cells (NSCs) (Rodriguez et al. 2012). MiR-31 expression was also striking in the trigeminal ganglion (TG) (Fig. 2A, iii and iv) (Schambra et al. 1991), and ventricular zones (VZ) and subventricular zones (SVZ) of the ganglionic eminence (GE) (Fig. 2A, v and vi). The TG is a mass of pseudounipolar neurons tightly enveloped by satellite glial cells (Erzurumlu et al. 2006; Viana 2011; Vit et al. 2006), while the VZ and SVZ of the GE host pools of proliferating progenitor cells (Zechel et al. 2014). These data demonstrate that miR-31 is expressed in host glial and progenitor cells during the neurogenic-to-gliogenic switch.

MicroRNA-31 is Elevated in Differentiated Astrocytes

To ascertain which cells in the CNS expressed miR-31, we analyzed Gene Expression Omnibus (GEO) datasets. In rat, we found miR-31 was significantly more abundant in

astrocytes compared to neurons, oligodendrocytes or microglia (GSE34614; Fig. 2B); in *homo sapiens*, miR-31 levels were elevated as astrocytes matured (GSE15888; Fig. 2C). To confirm these data, we compared miR-31 levels in primary murine astrocytes and NPCs; NPCs were isolated from E15 embryos and astrocytes isolated from newborn mice (P0). The murine neurogenic-gliogenic switch occurs at approximately E14.5, and afterwards NPCs are largely committed to producing astrocytes and oligodendrocytes (Martynoga et al. 2012; Sanosaka et al. 2008). Although miR-31 was detected in both cell types, the levels of miR-31 were significantly higher in astrocytes (Fig. 2D). The identity of NPCs and astrocytes were confirmed by qRT-PCR and flow cytometry using Olig2, Nestin and SOX2 as NPC markers and GFAP as a marker of astrocytes (data not shown). Collectively, these data indicate that the levels of miR-31 become elevated in the developing CNS, and that miR-31 expression is predominantly in astrocytes.

miR-31 is Induced During Differentiation

In order to assess the role of miR-31 during astrocytogenesis *in vitro*, E14.5 NPCs were cultured in the absence or presence of 10% FBS for 3 days in order to induce astrocyte differentiation (Obayashi et al. 2009). Without FBS, NPCs grow as loosely adherent cells (Fig. 3A, untreated; UT), and express SOX2 (stem cell marker), but only modest GFAP (astrocyte marker) (Fig. 3B, UT). After FBS treatment, NPCs adopt a flattened, adherent morphology (Fig. 3A, FBS), lose SOX2 reactivity and differentiate into $GFAP^+$ astrocytes (Fig. 3B, FBS). We confirmed that *GFAP* levels were significantly elevated, while those of stem cell markers were significantly reduced (Figs. 3C–E, G) via qRT-PCR and immunoblotting. The *GFAP* gene is expressed as multiple alternatively spliced isoforms (Fig. 3G) (Thomsen et al. 2013); presently, the significance of these other isoforms is not yet clear. Importantly, we determined miR-31 levels increased as NPCs differentiated into astrocytes (Fig. 3F). To confirm miR-31 levels increase regardless of the method used to differentiate NPCs into astrocytes, NPCs were left untreated (UT) or treated with LIF, BMP2, BMP2 + LIF, or FBS (Lee et al. 2008). Alone, LIF modestly increased miR-31 levels, while BMP2 alone or BMP2 + LIF increased miR-31 to levels comparable to cells treated with 10% FBS (Fig. 3H). The levels of miR-31 expression were positively correlated with GFAP expression, and inversely correlated with the levels of Lin28 (Fig. 3I). These data confirm miR-31 is induced during astrocyte differentiation.

miR-31 is Regulated by Transcription Factors that Regulate NPC-to-Astrocyte Differentiation

To understand what factors might regulate miR-31 expression, ECR Browser (www.ecrbrowser.dcode.org) compared mouse and human genomes to identify evolutionarily conserved regions (ECR) within the *MIR31HG* promoter; we identified six ECR (Fig. 3J, 1–6) upstream of the transcriptional start site (TSS) of *MIR31HG*; these ECRs are approximately 68–70% conserved between mouse and human. Contained within these regions were response elements for stem cell factors (Oct4 (ECR 1, 2, 3, 5), SOX2 (ECR 2, 4), c-Myc (ECR 3)) and transcription factors implicated in astrocyte development (STAT3 (ECR 2, 3, 4,) and SMAD1/5/8 (ECR 6). We used chromatin immunoprecipitation to determine if these transcription factors regulate miR-31 expression in NPCs and/or astrocytes. As such, NPCs were grown in the absence (UT) or presence of 10% FBS (FBS)

for 3 d as shown in Figs. 3A, B. The levels of c-Myc (Fig. 3K), SOX2 (Fig. 3L) and Oct4 (Fig. 3M) were elevated in the undifferentiated NPCs compared to FBS treated NPCs. Conversely, the levels of SMAD1/5/8 (Fig. 3N) and STAT3 (Fig. 3O) were increased by FBS-induced astrocytogenesis compared to NPCs. To correlate these events with active transcriptional events, we evaluated EZH2, a subunit of polycomb repressive complex 2 (PRC2), and tri-methylated lysine 27 of histone 3 (H3K27Me3), which marks transcriptionally silent DNA. The levels of both EZH2 (Fig. 3P) and H3K27Me3 (Fig. 3Q) were reduced by FBS treatment; these data indicate that the epigenomic environment near the *MIR31HG* promoter is less repressive after FBS treatment. Collectively, these data indicate miR-31 is repressed by stem cell factors in NPCs, and is induced by SMAD1/5/8 and STAT3 during astrocyte development.

Ectopic MiR-31 Expression Induces Partial Astrocyte Differentiation

To assess whether miR-31 promotes or merely coincides with astrocyte differentiation, NPCs were transfected with either control miR (CT) or miR-31; we confirmed miR-31 was expressed (Fig. 4A), and that this coincided with increased levels of GFAP mRNA (Fig. 4B) and protein (Fig. 4E), and reduced levels of Nestin and Lin28 (Figs. 4C–E); in Fig. 4E, multiple alternatively spliced GFAP isoforms are detected (Thomsen et al. 2013). Thus, exogenous miR-31 produces changes in gene expression associated with astrocyte differentiation. To assess whether miR-31 is required for astrocyte differentiation, NPCs were transfected with CT miR or AntagomiR-31, and then left untreated (UT) or differentiated into astrocytes using 10% FBS (FBS). FBS significantly increased the levels of miR-31 (Fig. 4F) and GFAP (Figs. 4G, H), and reduced the levels of Lin28 (Fig. 4H) in NPCs expressing CT miR. However, if miR-31 expression was blocked (Fig. 4F), changes indicative of astrocyte specification, including elevated and reduced levels of GFAP (Figs. 4G, H) and Lin28, respectively, (Fig. 4H) were impaired. Astrocytogenesis is accompanied by morphological changes including the formation of astrocytic processes (Bolego et al. 1997; Lippman et al. 2008). Therefore, we measured the length and counted the number of astrocytic processes in NPCs transfected with CT miR or miR-31 after 7 d. Cells transfected with miR-31 exhibited significantly more, but shorter, astrocytic processes per cell than those with CT miR (Figs. 4I, J). Collectively, these data suggest miR-31 can promote, in part, astrocyte development.

MiR-31 is Required for Astrocyte Specification

Next, we tested whether miR-31 is required for astrocyte specification. Normal murine astrocytes (P0) were transfected with CT miR or AntagomiR-31 (A) for 7 d, and then analyzed by immunofluorescence and immunoblotting. The levels of GFAP were significantly reduced in astrocytes that lacked miR-31 (Antagomir; A) (Fig. 5A, lower panel; Fig. 5B); additionally, cells appeared rounded in shape and there were fewer astrocytic processes per cell (data not shown). Interestingly, we found the loss of miR-31 correlated with increased levels of KLF4, SOX2, Oct4 and Nestin (Fig. 5B). The loss of miR-31 alone only modestly increased Lin28 levels (Fig. 5C); this suggests that while the loss of miR-31 may sufficiently stabilize Lin28 levels, it cannot induce *de novo Lin28* expression. To assess how the loss of miR-31 impacts stimulus-induced (IL-1β) Lin28 expression, cells were transfected with CT or A for 48 hr, and then grown in the absence or presence of IL-1β; this

activates NF-κB and increases the levels of both Lin28 (Iliopoulos et al. 2009) and miR-31 (Rajbhandari et al. 2015). NF-κB induced Lin28 expression was more pronounced in cells that lack miR-31 (A) compared to those that express miR-31 (UT) (Fig. 5C).

Next, we evaluated how the loss of miR-31 might impact the health of astrocytes; cells were transfected with CT miR (CT), miR-31 or AntagomiR-31 for various times (0–9 days) and cell metabolism was evaluated using the WST-1 assay. The metabolic profiles of astrocytes transfected with CT or miR-31 were nearly indistinguishable, suggesting CT and miR-31 did not adversely astrocytic health (Fig. 5D). Conversely, the metabolism of astrocytes lacking miR-31 (AntagomiR) was significantly reduced (Fig. 5D), and this coincided with loss of astrocytic processes and attachment as noted above (Fig. 5A, data not shown). These data suggest that loss of miR-31 in astrocytes may prevent astrocyte maturation and adversely impact the health of astrocytes.

Loss of Lin28 Expression Promotes Astrocyte Development

MiR targets mRNA to reduce gene expression; therefore, we reasoned miR-31 may target 1 or more stem cell factors to promote astrocyte differentiation. Above, we determined the levels of miR-31 were inversely correlated with Lin28, Oct4, SOX2 and C-myc; of these, only the *Lin28* mRNA contained three miR-31 elements (Fig. 6A). Immunoblots confirmed that the levels of Lin28 (Fig. 6B) inversely correlated with levels of miR-31 (Fig. 3F) in NPCs and astrocytes. To test whether the 3′ UTR of Lin28 was responsive to miR-31, the Lin28 3′ UTR (Lin28) or control DNA was inserted downstream of the luciferase (Luc) gene. Next, U251-MG astroglioma cells, which express miR-31, were transfected with control miR (CT) or AntagomiR-31 (Ant-31) for 48 h, and then transfected with either control or Lin28-Luc for an additional 24 h. In U251-MG cells, loss of miR-31 expression significantly enhanced Lin28-Luc activity (Fig. 6C). We also transfected U87-MG astroglioma cells, which lack miR-31 expression, with CT or miR-31, and then CT-Luc or Lin28-Luc, as described above. In U87-MG cells, miR-31 significantly reduced the levels of Lin28-Luc but not CT-Luc (Fig. 6D). These data indicate that the 3′ UTR of Lin28 is responsive to miR-31.

To test whether miR-31 targets Lin28 in order to promote astrocytogenesis, NPCs were transfected with CT miRNA (CT), miR-31, shRNA specific for Lin28 (shLin28), or miR-31 + shLin28 (31 + sh). For comparison, NPCs were grown in the presence of 10% FBS or 10% FBS + miR-31 + shLin28 (FBS + 31 + sh). In the presence of CT miR, NPCs grow as loosely adherent neurospheres (Fig. 7A, CT) that express Lin28 (Fig. 7C) and minimal miR-31 (Fig. 7B). After 3 d of 10% FBS, NPCs adopt the flattened morphology of astrocytes (Fig. 7A, FBS), and express elevated and reduced levels of miR-31 (Fig. 7B) and Lin28 (Fig. 7C), respectively. NPCs transfected with miR-31 alone (Fig. 7B) also exhibited reduced Lin28 expression (Fig. 7C), and this coincided with loss of neurosphere formation and growth as adherent, astrocyte-like cells (Fig. 7A, miR-31). Interestingly, loss of Lin28 expression alone (shLin28) significantly elevated endogenous miR-31 levels (Fig. 7B, compare shLin28 and CT). Lin28 expression was most effectively reduced if miR-31 expression was combined with shLin28, either in the absence and presence of FBS (Fig.

7C). These data suggest that miR-31 induces astrocyte development, in part, by suppressing Lin28 levels, and that Lin28 may negatively regulate miR-31 expression.

We hypothesized that Lin28 and miR-31 may antagonize one another's expression in order to promote NPC maintenance (Lin28) or astrocyte development (miR-31). Lin28 is an RNA-binding protein; to test if Lin28 directly bound miR-31, cells were grown in the absence or presence of TNF-α (TNF) to activate NF-κB(Iliopoulos et al. 2009; Pomerantz and Baltimore 1999), and RNA-immunoprecipitation (RIP)/qRT-PCR assays were performed. These studies were performed in U251-MG cells as they constitutively express miR-31; moreover, TNF-α induced NF-κB further elevates the levels of Lin28 expression and miR-31 (Iliopoulos et al. 2009; Rajbhandari et al. 2015). Equal amounts of protein were immunoprecipitated (IP'd) with control antibodies (IgG) or antibodies specific for Lin28 (Lin28), and co-IP'd RNA was purified and analyzed for miR-31 using qRT-PCR. As shown in Fig. 7D, miR-31 associated with Lin28, but not control IgG. When bound to Lin28, miRs are not free to bind target mRNA; these data suggest that Lin28 may "soak-up" any residual miR-31 levels in order to prevent NPC to astrocyte differentiation.

Discussion

Herein, we present data demonstrating the temporal and spatial expression pattern of miR-31 within the developing CNS. We find miR-31 is expressed in most cells of the developing CNS, but its levels are most profound in astrocytes. We find NPCs utilize stem cell transcription factors to block the miR-31 promoter in order to maintain low levels of miR-31; additionally, NPCs modify DNA and histones (EZH2, H3K27Me3) to inhibit miR-31 transcription. Should any residual miR-31 be expressed, we found that the RNA-binding protein Lin28 bound to and inhibited miR-31 (Fig. 8). From these data, we can speculate that miR-31 expression and/or activity must be blocked in NPCs in order to avoid premature astrocytogenesis. Indeed, during astrocyte specification, STAT3 and BMP1/5/8 become activated and bind to the miR-31 promoter; this coincides with diminished levels of suppressive factors and motifs, and correlates with an increase in the levels of miR-31. The ChIP data directly demonstrate that STAT3 and BMP1/5/8 drive miR-31 expression during astrocytogenesis. We demonstrate miR-31 is a key player during astrocyte specification. Alone, miR-31 is competent to partially induce astrocytogenesis; conversely, in the absence of miR-31, NPCs are unable to completely differentiate into astrocytes. From these data, we hypothesize that miR-31 is important for directly promoting astrocyte differentiation. In mature astrocytes, we determined the loss of miR-31 induced morphological and phenotypic changes that altered cellular phenotype and permitted markers of earlier developmental stages to be expressed. These data suggest miR-31 may be required to "lock" astrocytes into this identity. Finally, we determine miR-31 targets the stem cell factor and RNA-binding protein Lin28; additionally, miR-31 may promote astrocyte development, in part, by suppressing Lin28 expression.

Astrocytes are the most abundant cell type in the mammalian CNS (Namihira and Nakashima 2013). In mice, astrocyte production begins after the neurogenic-to-gliogenic switch, but is most prominent at P0–P14 (Nakayama et al. 2006; Setoguchi et al. 2006; Yanagisawa et al. 2000; Yanagisawa et al. 2001). Astrocytes provide structural support,

maintain water balance and ion distribution, and help establish the blood-brain barrier (BBB) (Namihira and Nakashima 2013). During injury or disease, astrocytes help restore homeostasis to the microenvironment (Gallo and Deneen 2014). Astrocytes have been implicated in nearly all cases of CNS injury, degeneration and disease (Gallo and Deneen 2014). However, exactly how NPCs differentiate into astrocytes is not fully known.

Several transcription factors, including NFIA, STAT3 and SMAD1/5/8, have been implicated in astrocytogenesis (Glasgow et al. 2013; Glasgow et al. 2014a; Lee et al. 2014; Urayama et al. 2013; Yanagisawa et al. 2000). However, few studies have addressed the role of non-coding factors, such as miRs, and their potential contribution towards astrocytogenesis (Cacci et al. 2017; Jovicic and Gitler 2017; Karthikeyan et al. 2016; Li et al. 2016; Rao et al. 2016; Smith et al. 2010; Yun et al. 2010). By comparison, more is known about the contributions of miRs during neurogenesis (Boutz et al. 2007; Choi et al. 2008; Hobert 2006; Johnston et al. 2005; Kuss and Chen 2008; Makeyev et al. 2007; Sempere et al. 2004). Therefore, our study is significant as it identifies miR-31 as a potent mediator of astrocyte development. In our previous work, we determined that one or more alleles of miR-31 is deleted in GBM (Rajbhandari et al. 2015). We hypothesize that the loss of miR-31 prevents normal astrocyte development and likely contributes to and/or worsens GBM tumorigencity (Rajbhandari et al. 2015). Our studies also highlight the important role cell-specific miRs mediate during lineage specification, and underscore the need to determine whether these miRs are involved in disease formation/progression. Ideally, other investigators and future studies will help address the role(s) of miRs in astrocyte development and disease.

Acknowledgments

Funding for this work was provided by grants from the National Multiple Sclerosis Society (TA3050-A-1 to G.P.M), National Institutes of Health (R01CA158534 and R01CA194414 to E.N.B., R01CA138517 to S.E.N., 5T32NS048039-08 to S.C.F. and A.R., and R01GM098566 to C.C.); and a Faculty Development Grant from the UAB Comprehensive Cancer Center to M.B. and S.E.N..

Bibliography

Aloia L, Di Stefano B, Di Croce L. Polycomb complexes in stem cells and embryonic development. Development. 2013; 140:2525–34. [PubMed: 23715546]

Alvarez-Buylla A, Garcia-Verdugo JM, Tramontin AD. A unified hypothesis on the lineage of neural stem cells. Nat Rev Neurosci. 2001; 2:287–93. [PubMed: 11283751]

Bolego C, Ceruti S, Brambilla R, Puglisi L, Cattabeni F, Burnstock G, Abbracchio MP. Characterization of the signalling pathways involved in ATP and basic fibroblast growth factor-induced astrogliosis. Br J Pharmacol. 1997; 121:1692–9. [PubMed: 9283705]

Bonev B, Papalopulu N. Methods to analyze microRNA expression and function during Xenopus development. Methods in Molecular Biology. 2012; 917:445–59. [PubMed: 22956103]

Boutz PL, Chawla G, Stoilov P, Black DL. MicroRNAs regulate the expression of the alternative splicing factor nPTB during muscle development. Genes Dev. 2007; 21:71–84. [PubMed: 17210790]

Cacci E, Negri R, Biagioni S, Lupo G. Histone Methylation and microRNA-dependent Regulation of Epigenetic Activities in Neural Progenitor Self-Renewal and Differentiation. Curr Top Med Chem. 2017; 17:794–807. [PubMed: 27086782]

Chaker Z, Codega P, Doetsch F. A mosaic world: puzzles revealed by adult neural stem cell heterogeneity. Wiley Interdiscip Rev Dev Biol. 2016; 5:640–658. [PubMed: 27647730]

Choi PS, Zakhary L, Choi WY, Caron S, Alvarez-Saavedra E, Miska EA, McManus M, Harfe B, Giraldez AJ, Horvitz HR, et al. Members of the miRNA-200 family regulate olfactory neurogenesis. Neuron. 2008; 57:41–55. [PubMed: 18184563]

Deneen B, Ho R, Lukaszewicz A, Hochstim CJ, Gronostajski RM, Anderson DJ. The transcription factor NFIA controls the onset of gliogenesis in the developing spinal cord. Neuron. 2006; 52:953–68. [PubMed: 17178400]

Dietrich J, Imitola J, Kesari S. Mechanisms of disease: the role of stem cells in the biology and treatment of gliomas. Nature Clinical Practice Oncology. 2008; 5:393–404.

Dirks PB. Cancer: stem cells and brain tumours. Nature. 2006; 444:687–8. [PubMed: 17151644]

Erzurumlu RS, Chen ZF, Jacquin MF. Molecular determinants of the face map development in the trigeminal brainstem. Anat Rec A Discov Mol Cell Evol Biol. 2006; 288:121–34. [PubMed: 16432893]

Fukuda S, Abematsu M, Mori H, Yanagisawa M, Kagawa T, Nakashima K, Yoshimura A, Taga T. Potentiation of astrogliogenesis by STAT3-mediated activation of bone morphogenetic protein-Smad signaling in neural stem cells. Molecular and Cellular Biology. 2007; 27:4931–7. [PubMed: 17452461]

Gallo V, Deneen B. Glial development: the crossroads of regeneration and repair in the CNS. Neuron. 2014; 83:283–308. [PubMed: 25033178]

Glasgow SM, Laug D, Brawley VS, Zhang Z, Corder A, Yin Z, Wong ST, Li XN, Foster AE, Ahmed N, et al. The miR-223/nuclear factor I-A axis regulates glial precursor proliferation and tumorigenesis in the CNS. J Neurosci. 2013; 33:13560–8. [PubMed: 23946414]

Glasgow SM, Zhu W, Stolt CC, Huang TW, Chen F, LoTurco JJ, Neul JL, Wegner M, Mohila C, Deneen B. Mutual antagonism between Sox10 and NFIA regulates diversification of glial lineages and glioma subtypes. Nat Neurosci. 2014a; 17:1322–9. [PubMed: 25151262]

Glasgow SM, Zhu W, Stolt CC, Huang TW, Chen F, LoTurco JJ, Neul JL, Wegner M, Mohila C, Deneen B. Mutual antagonism between Sox10 and NFIA regulates diversification of glial lineages and glioma subtypes. Nature Neuroscience. 2014b; 17:1322–9. [PubMed: 25151262]

Harland RM. In situ hybridization: an improved whole-mount method for Xenopus embryos. Methods in Cell Biology. 1991; 36:685–95. [PubMed: 1811161]

Hobert O. Architecture of a microRNA-controlled gene regulatory network that diversifies neuronal cell fates. Cold Spring Harb Symp Quant Biol. 2006; 71:181–8. [PubMed: 17381295]

Iliopoulos D, Hirsch HA, Struhl K. An epigenetic switch involving NF-kappaB, Lin28, Let-7 MicroRNA, and IL6 links inflammation to cell transformation. Cell. 2009; 139:693–706. [PubMed: 19878981]

Johnston RJ Jr, Chang S, Etchberger JF, Ortiz CO, Hobert O. MicroRNAs acting in a double-negative feedback loop to control a neuronal cell fate decision. Proc Natl Acad Sci U S A. 2005; 102:12449–54. [PubMed: 16099833]

Jovicic A, Gitler AD. Distinct repertoires of microRNAs present in mouse astrocytes compared to astrocyte-secreted exosomes. PLoS One. 2017; 12:e0171418. [PubMed: 28152040]

Kang P, Lee HK, Glasgow SM, Finley M, Donti T, Gaber ZB, Graham BH, Foster AE, Novitch BG, Gronostajski RM, et al. Sox9 and NFIA coordinate a transcriptional regulatory cascade during the initiation of gliogenesis. Neuron. 2012; 74:79–94. [PubMed: 22500632]

Karthikeyan A, Patnala R, Jadhav SP, Eng-Ang L, Dheen ST. MicroRNAs: Key Players in Microglia and Astrocyte Mediated Inflammation in CNS Pathologies. Curr Med Chem. 2016; 23:3528–3546. [PubMed: 27528056]

Kim TM, Huang W, Park R, Park PJ, Johnson MD. A developmental taxonomy of glioblastoma defined and maintained by microRNAs. Cancer Research. 2011; 71:3387–99. [PubMed: 21385897]

Koemeter-Cox AI, Sherwood TW, Green JA, Steiner RA, Berbari NF, Yoder BK, Kauffman AS, Monsma PC, Brown A, Askwith CC, et al. Primary cilia enhance kisspeptin receptor signaling on gonadotropin-releasing hormone neurons. Proc Natl Acad Sci U S A. 2014; 111:10335–40. [PubMed: 24982149]

Kuss AW, Chen W. MicroRNAs in brain function and disease. Curr Neurol Neurosci Rep. 2008; 8:190–7. [PubMed: 18541114]

Lee J, Son MJ, Woolard K, Donin NM, Li A, Cheng CH, Kotliarova S, Kotliarov Y, Walling J, Ahn S, et al. Epigenetic-mediated dysfunction of the bone morphogenetic protein pathway inhibits differentiation of glioblastoma-initiating cells. Cancer Cell. 2008; 13:69–80. [PubMed: 18167341]

Lee JS, Xiao J, Patel P, Schade J, Wang J, Deneen B, Erdreich-Epstein A, Song HR. A novel tumor-promoting role for nuclear factor IA in glioblastomas is mediated through negative regulation of p53, p21, and PAI1. Neuro Oncol. 2014; 16:191–203. [PubMed: 24305710]

Li X, Chen Y, Chi Q, Hu X, Xu X, Zhang Z, Qiu M, Zheng K. miRNAs are required for the terminal differentiation of white matter astrocytes in the developing CNS. Neuroscience. 2016; 312:99–107. [PubMed: 26556063]

Lippman JJ, Lordkipanidze T, Buell ME, Yoon SO, Dunaevsky A. Morphogenesis and regulation of Bergmann glial processes during Purkinje cell dendritic spine ensheathment and synaptogenesis. Glia. 2008; 56:1463–77. [PubMed: 18615636]

Liu Y, Wu Y, Lee JC, Xue H, Pevny LH, Kaprielian Z, Rao MS. Oligodendrocyte and astrocyte development in rodents: an in situ and immunohistological analysis during embryonic development. Glia. 2002; 40:25–43. [PubMed: 12237841]

Loh YH, Wu Q, Chew JL, Vega VB, Zhang W, Chen X, Bourque G, George J, Leong B, Liu J, et al. The Oct4 and Nanog transcription network regulates pluripotency in mouse embryonic stem cells. Nature Genetics. 2006; 38:431–40. [PubMed: 16518401]

Lujambio A, Lowe SW. The microcosmos of cancer. Nature. 2012; 482:347–55. [PubMed: 22337054]

Makeyev EV, Zhang J, Carrasco MA, Maniatis T. The MicroRNA miR-124 promotes neuronal differentiation by triggering brain-specific alternative pre-mRNA splicing. Mol Cell. 2007; 27:435–48. [PubMed: 17679093]

Maldonado-Soto AR, Oakley DH, Wichterle H, Stein J, Doetsch FK, Henderson CE. Stem cells in the nervous system. Am J Phys Med Rehabil. 2014; 93:S132–44. [PubMed: 24800720]

Martynoga B, Drechsel D, Guillemot F. Molecular control of neurogenesis: a view from the mammalian cerebral cortex. Cold Spring Harb Perspect Biol. 2012:4.

McFarland BC, Hong SW, Rajbhandari R, Twitty GB Jr, Gray GK, Yu H, Benveniste EN, Nozell SE. NF-kappaB-induced IL-6 ensures STAT3 activation and tumor aggressiveness in glioblastoma. PLoS One. 2013; 8:e78728. [PubMed: 24244348]

Meares GP, Liu Y, Rajbhandari R, Qin H, Nozell SE, Mobley JA, Corbett JA, Benveniste EN. PERK-dependent activation of JAK1 and STAT3 contributes to endoplasmic reticulum stress-induced inflammation. Mol Cell Biol. 2014; 34:3911–25. [PubMed: 25113558]

Meares GP, Qin H, Liu Y, Holdbrooks AT, Benveniste EN. AMP-activated protein kinase restricts IFN-gamma signaling. Journal of Immunology. 2013; 190:372–80.

Molofsky AV, Krencik R, Ullian EM, Tsai HH, Deneen B, Richardson WD, Barres BA, Rowitch DH. Astrocytes and disease: a neurodevelopmental perspective. Genes & Development. 2012; 26:891–907. [PubMed: 22549954]

Nakayama T, Sai T, Otsu M, Momoki-Soga T, Inoue N. Astrocytogenesis of embryonic stem-cell-derived neural stem cells: Default differentiation. Neuroreport. 2006; 17:1519–23. [PubMed: 16957601]

Namihira M, Nakashima K. Mechanisms of astrocytogenesis in the mammalian brain. Curr Opin Neurobiol. 2013; 23:921–7. [PubMed: 23827784]

Nie S, Chang C. Regulation of Xenopus gastrulation by ErbB signaling. Developmental Biology. 2007; 303:93–107. [PubMed: 17134691]

Noctor SC, Flint AC, Weissman TA, Dammerman RS, Kriegstein AR. Neurons derived from radial glial cells establish radial units in neocortex. Nature. 2001; 409:714–20. [PubMed: 11217860]

Nozell S, Laver T, Moseley D, Nowoslawski L, De Vos M, Atkinson GP, Harrison K, Nabors LB, Benveniste EN. The ING4 tumor suppressor attenuates NF-kappaB activity at the promoters of target genes. Molecular and Cellular Biology. 2008; 28:6632–45. [PubMed: 18779315]

Obayashi S, Tabunoki H, Kim SU, Satoh J. Gene expression profiling of human neural progenitor cells following the serum-induced astrocyte differentiation. Cellular and Molecular Neurobiology. 2009; 29:423–38. [PubMed: 19130216]

Paul A, Chaker Z, Doetsch F. Hypothalamic regulation of regionally distinct adult neural stem cells and neurogenesis. Science. 2017; 356:1383–1386. [PubMed: 28619719]

Pomerantz JL, Baltimore D. NF-kappaB activation by a signaling complex containing TRAF2, TANK and TBK1, a novel IKK-related kinase. EMBO Journal. 1999; 18:6694–704. [PubMed: 10581243]

Rajbhandari R, McFarland BC, Patel A, Gerigk M, Gray GK, Fehling SC, Bredel M, Berbari NF, Kim H, Marks MP, et al. Loss of tumor suppressive microRNA-31 enhances TRADD/NF-kappaB signaling in glioblastoma. Oncotarget. 2015; 6:17805–16. [PubMed: 26164206]

Rao VT, Ludwin SK, Fuh SC, Sawaya R, Moore CS, Ho MK, Bedell BJ, Sarnat HB, Bar-Or A, Antel JP. MicroRNA Expression Patterns in Human Astrocytes in Relation to Anatomical Location and Age. J Neuropathol Exp Neurol. 2016; 75:156–66. [PubMed: 26802178]

Rodriguez EM, Guerra MM, Vio K, Gonzalez C, Ortloff A, Batiz LF, Rodriguez S, Jara MC, Munoz RI, Ortega E, et al. A cell junction pathology of neural stem cells leads to abnormal neurogenesis and hydrocephalus. Biol Res. 2012; 45:231–42. [PubMed: 23283433]

Ronan JL, Wu W, Crabtree GR. From neural development to cognition: unexpected roles for chromatin. Nature Reviews Genetics. 2013; 14:347–59.

Sanosaka T, Namihira M, Asano H, Kohyama J, Aisaki K, Igarashi K, Kanno J, Nakashima K. Identification of genes that restrict astrocyte differentiation of midgestational neural precursor cells. Neuroscience. 2008; 155:780–8. [PubMed: 18640244]

Schambra UB, Silver J, Lauder JM. An atlas of the prenatal mouse brain: gestational day 14. Exp Neurol. 1991; 114:145–83. [PubMed: 1748192]

Schroeder TE. Neurulation in Xenopus laevis. An analysis and model based upon light and electron microscopy. Journal of Embryology and Experimental Morphology. 1970; 23:427–62. [PubMed: 5449482]

Sempere LF, Freemantle S, Pitha-Rowe I, Moss E, Dmitrovsky E, Ambros V. Expression profiling of mammalian microRNAs uncovers a subset of brain-expressed microRNAs with possible roles in murine and human neuronal differentiation. Genome Biol. 2004; 5:R13. [PubMed: 15003116]

Setoguchi H, Namihira M, Kohyama J, Asano H, Sanosaka T, Nakashima K. Methyl-CpG binding proteins are involved in restricting differentiation plasticity in neurons. J Neurosci Res. 2006; 84:969–79. [PubMed: 16881068]

Shyh-Chang N, Daley GQ. Lin28: primal regulator of growth and metabolism in stem cells. Cell Stem Cell. 2013; 12:395–406. [PubMed: 23561442]

Sieber C, Kopf J, Hiepen C, Knaus P. Recent advances in BMP receptor signaling. Cytokine & Growth Factor Reviews. 2009; 20:343–55. [PubMed: 19897402]

Smith B, Treadwell J, Zhang D, Ly D, McKinnell I, Walker PR, Sikorska M. Large-scale expression analysis reveals distinct microRNA profiles at different stages of human neurodevelopment. PLoS One. 2010; 5:e11109. [PubMed: 20559549]

Thomsen R, Daugaard TF, Holm IE, Nielsen AL. Alternative mRNA splicing from the glial fibrillary acidic protein (GFAP) gene generates isoforms with distinct subcellular mRNA localization patterns in astrocytes. PLoS One. 2013; 8:e72110. [PubMed: 23991052]

Tien CL, Jones A, Wang H, Gerigk M, Nozell S, Chang C. Snail2/Slug cooperates with Polycomb repressive complex 2 (PRC2) to regulate neural crest development. Development. 2015; 142:722–31. [PubMed: 25617436]

Tiwari N, Tiwari VK, Waldmeier L, Balwierz PJ, Arnold P, Pachkov M, Meyer-Schaller N, Schubeler D, van Nimwegen E, Christofori G. Sox4 is a master regulator of epithelial-mesenchymal transition by controlling Ezh2 expression and epigenetic reprogramming. Cancer Cell. 2013; 23:768–83. [PubMed: 23764001]

Tome-Garcia J, Tejero R, Nudelman G, Yong RL, Sebra R, Wang H, Fowkes M, Magid M, Walsh M, Silva-Vargas V, et al. Prospective Isolation and Comparison of Human Germinal Matrix and Glioblastoma EGFR+ Populations with Stem Cell Properties. Stem Cell Reports. 2017; 8:1421–1429. [PubMed: 28434940]

Urayama S, Semi K, Sanosaka T, Hori Y, Namihira M, Kohyama J, Takizawa T, Nakashima K. Chromatin accessibility at a STAT3 target site is altered prior to astrocyte differentiation. Cell Struct Funct. 2013; 38:55–66. [PubMed: 23439558]

Viana F. Chemosensory properties of the trigeminal system. ACS Chem Neurosci. 2011; 2:38–50. [PubMed: 22778855]

Vit JP, Jasmin L, Bhargava A, Ohara PT. Satellite glial cells in the trigeminal ganglion as a determinant of orofacial neuropathic pain. Neuron Glia Biol. 2006; 2:247–57. [PubMed: 18568096]

Yanagisawa M, Nakashima K, Arakawa H, Ikenaka K, Yoshida K, Kishimoto T, Hisatsune T, Taga T. Astrocyte differentiation of fetal neuroepithelial cells by interleukin-11 via activation of a common cytokine signal transducer, gp130, and a transcription factor, STAT3. J Neurochem. 2000; 74:1498–504. [PubMed: 10737606]

Yanagisawa M, Takizawa T, Ochiai W, Uemura A, Nakashima K, Taga T. Fate alteration of neuroepithelial cells from neurogenesis to astrocytogenesis by bone morphogenetic proteins. Neurosci Res. 2001; 41:391–6. [PubMed: 11755226]

Yun SJ, Byun K, Bhin J, Oh JH, Nhung le TH, Hwang D, Lee B. Transcriptional regulatory networks associated with self-renewal and differentiation of neural stem cells. J Cell Physiol. 2010; 225:337–47. [PubMed: 20607797]

Zechel S, Zajac P, Lonnerberg P, Ibanez CF, Linnarsson S. Topographical transcriptome mapping of the mouse medial ganglionic eminence by spatially resolved RNA-seq. Genome Biol. 2014; 15:486. [PubMed: 25344199]

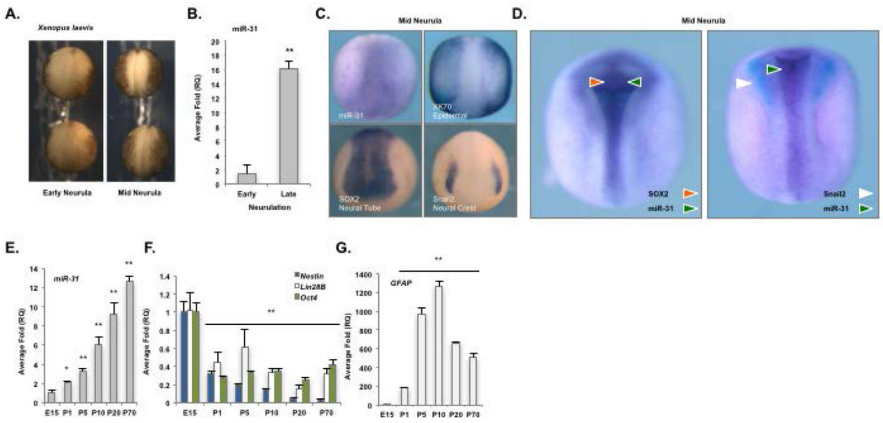

Fig. 1. MiR-31 is Induced During Neurogenesis

A. *Xenopus laevis* embryos at early and mid neurula stages of development. **B.** miR-31 levels from embryos (n=5) described in **(A)** were analyzed by qRT-PCR. (**, $p < 0.001$). Representative of two experiments. **C.** miR-31 expression at discrete developmental stages was analyzed in *X. laevis* embryos using ISH. The following genes were used as tissue specific markers: *XK70* (epidermal), *SOX2* (neural tube), and *Snail2* (neural crest). Data are representative of two experiments. **D.** miR-31 and *SOX2* or *Snail2* expression at discrete developmental stages were evaluated in *X. laevis* embryos using double ISH. Data are representative of two experiments. **E–G.** RNA levels from whole murine brains at developmental stages indicated (E15–P70) were analyzed by qRT-PCR. (*, $p < 0.05$; **, $p < 0.001$).

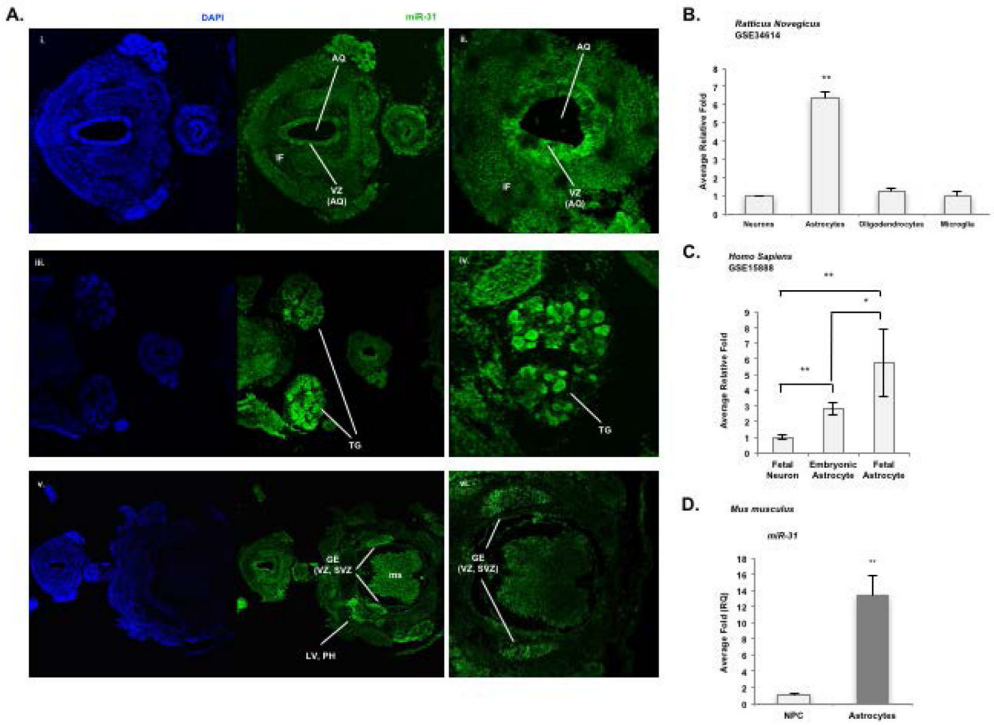

Fig. 2. MiR-31 is Preferentially Expressed in Developing Gliogenic Regions and Astrocytes

A. MiR-31 expression was analyzed in E14.5 murine brains using ISH; adjacent sections were stained with DAPI. (i and ii) IF – infundibulum, AQ – Aqueduct of Sylvius, VZ – ventricular zone; (iii and iv) TG – Trigeminal ganglion; (v and vi) GE – Ganglionic Eminence, SVZ – subventricular zone. **B, C.** The levels of miR-31 from purified *Ratticus novegicus* and *Homo sapiens* samples were analyzed from indicated Gene Expression Omnibus (GEO) sets specified. (*, $p < 0.05$; **, $p < 0.001$). **D.** RNA levels from purified murine NPCs (E14.5) or astrocytes (P0) were analyzed by qRT-PCR. (**, $p < 0.001$).

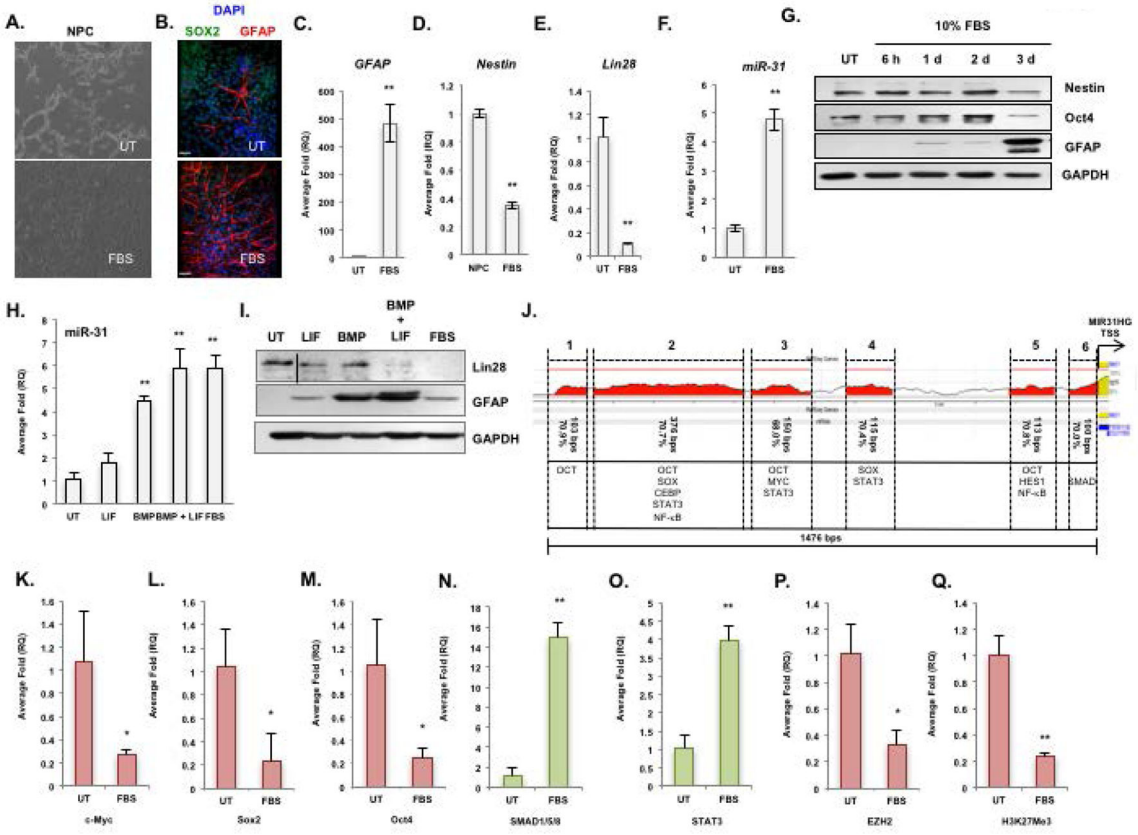

Fig. 3. MiR-31 Expression Correlates with Astrocyte Development

A–G. Murine NPCs (E14.5) were grown in the absence or presence of 10% FBS for three days to induce astrocyte differentiation. **A.** Light microscopy of NPCs grown in the absence (UT) or presence of 10% FBS (FBS). **B.** Immunofluorescence of NPCs grown as described in **(A)** using antibodies specific for SOX2 (stem cell marker; green) or GFAP (astrocyte marker; red). Nuclei were counterstained with DAPI. **C–F.** RNA from NPCs grown as described in **(A)** was analyzed by qRT-PCR. (**, $p < 0.001$). **G.** Protein levels from cells grown as described in **(A)** were analyzed by immunoblotting using the antibodies specified. **H, I.** NPCs (E14.5) were grown in the absence (UT) or presence of LIF (10 ng/ml), BMP2 (10 ng/ml), LIF plus BMP or 10% FBS for 3 days to induce astrocyte differentiation. **H.** RNA levels from NPCs grown as described above were evaluated by qRT-PCR. (**, $p < 0.001$). **I.** Protein levels from cells grown as described above were evaluated by immunoblotting using the antibodies specified. **J.** The miR-31 promoter spans 1,476 bp and contains six (1–6) evolutionarily conserved regions (ECRs) (indicated in red) upstream of the transcriptional start site (TSS). Below each ECR is the size in bps, percent homology between murine and human sequences, and putative transcription factor binding sites present in each area. **K–Q.** Normal murine NPCs (E14.5) were grown in the absence (UT) or presence of 10% FBS to induce astrocyte development, and ChIP assays were performed using the antibodies indicated. Samples were evaluated by qRT-PCR. (*, $p < 0.05$; **, $p < 0.001$).

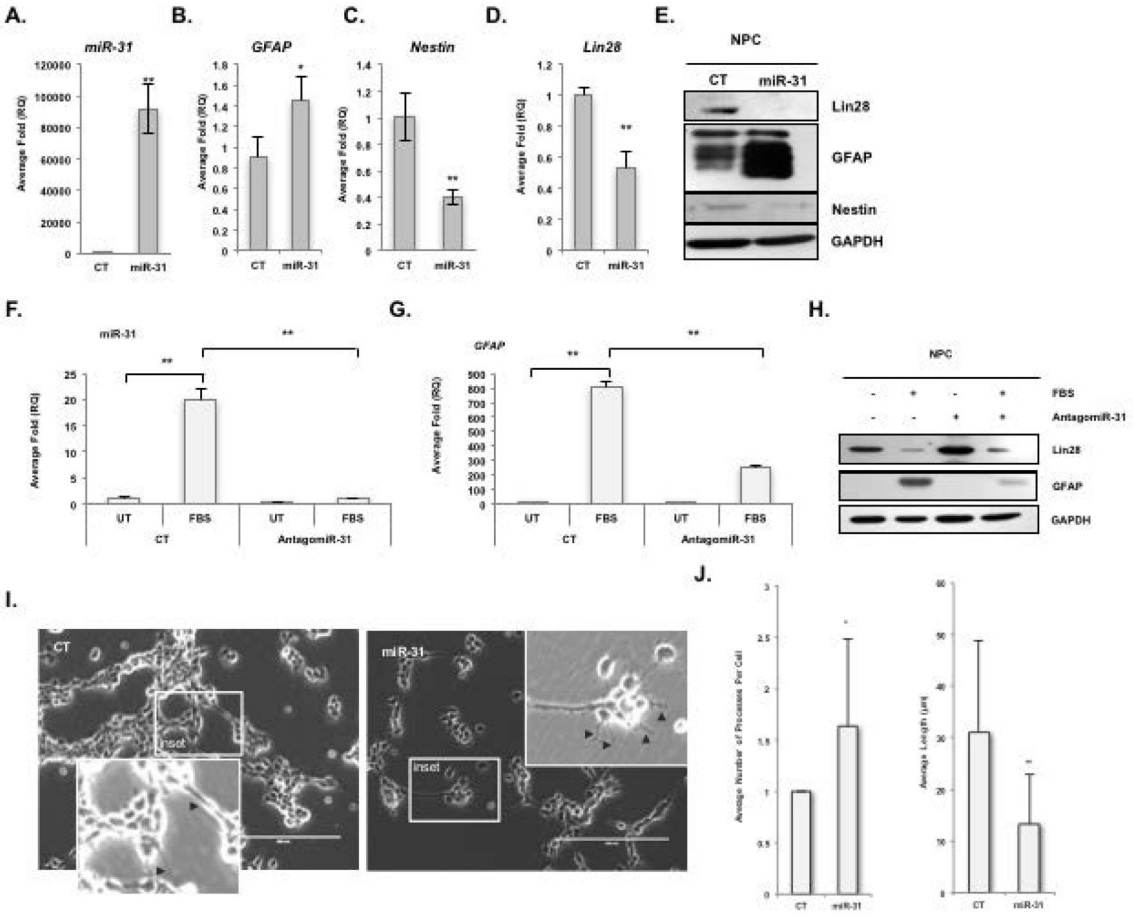

Fig. 4. MiR-31 Promotes Astrocyte Development

A–E. Murine NPCs (E14.5) were transfected with control (CT) or miR-31 for 48 h. **A–D.** RNA levels were analyzed by qRT-PCR. (*, $p < 0.05$; **, $p < 0.001$). **E.** Protein levels from cells grown as described above were evaluated by immunoblotting using the antibodies specified. **F–H.** NPCs were transfected with CT or AntagomiR-31 for 48 h, and then grown in the absence (UT) or presence of 10% FBS for an additional 3 d to induce astrocyte differentiation. **F, G.** RNA levels were analyzed by qRT-PCR. (**, $p < 0.001$). **H.** Protein levels in cells grown as described above were analyzed by immunoblotting using the antibodies specified. **I.** Light microscopy of cells grown under conditions described in (A). **J.** The number and length of astrocytic processes from cells grown as described in (A) and shown in (I) were assesssed; 50 cells per field were counted, and experiments were repeated three times. (*, $p < 0.05$).

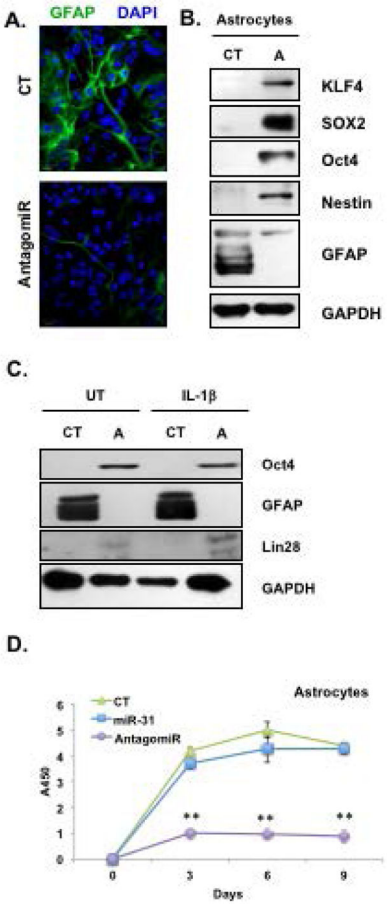

Fig. 5. Astrocytes Partially De-Differentiatie Upon Loss of miR-31

A, B. Primary murine astrocytes (P0) were transfected with control (CT) or AntagomiR-31 (AntagomiR/A) for 7 d. **A.** IF of cells grown as described above using antibodies specific for GFAP (astrocyte marker). Nuclei were counterstained with DAPI. **B.** Cells were grown as described above, and analyzed by immunoblotting using antibodies specific for stem cell markers (KLF4, SOX2, Oct4), NPCs (Nestin), astrocytes (GFAP) or GAPDH. **C.** Astrocytes were transfected with CT or AntagomiR-31 (A) and then grown in the absence or presence of IL-1β (5 ng/ml) for 7 d. IL-1β was used to activate NF-κB and induce Lin28 expression. Immunoblot analyses were performed using the antibodies specified. **D.** Murine astrocytes were transfected with control miR (CT), miR-31 or AntagomiR-31 and cell metabolism assessed at the days indicated using the WST1 assay. (**, $p < 0.001$).

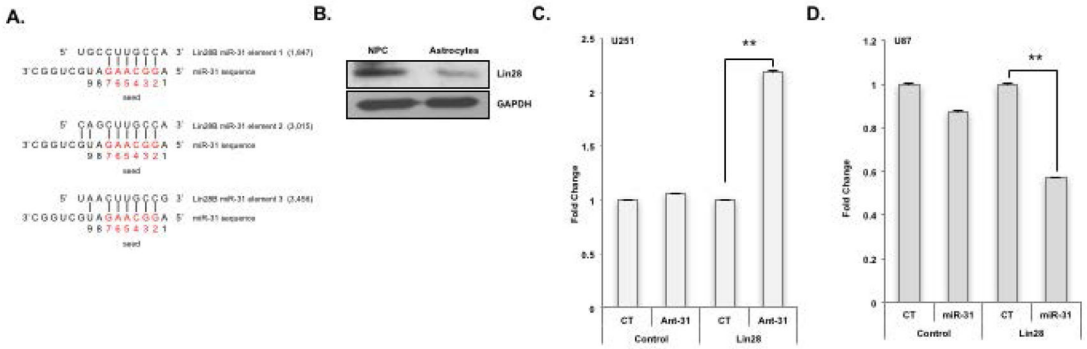

Fig. 6. MiR-31 Targets the Lin28 3′ UTR

A. The 3′ UTR of Lin28 contains three (1–3) putative miR-31 elements. The sequence of miR-31 is shown below each, with red indicating miR-31′s seed sequence. **B.** The level of Lin28 protein in murine NPCs and astrocytes was assessed by immunoblotting. **C.** U251-MG cells were transfected with a luciferase expression plasmid containing a control 3′ UTR (Control) or the 3′ UTR of Lin28 (Lin28), and either control miR (CT) or AntagomiR-31, and luciferase activity was analyzed. (**, $p < 0.001$). **D.** U87-MG cells were transfected with luciferase expression plasmid containing a control 3′ UTR (Control) or the 3′ UTR of Lin28 (Lin28), and either control miR (CT) or miR-31, and luciferase activity was analyzed. (**, $p < 0.001$). Representative of three experiments.

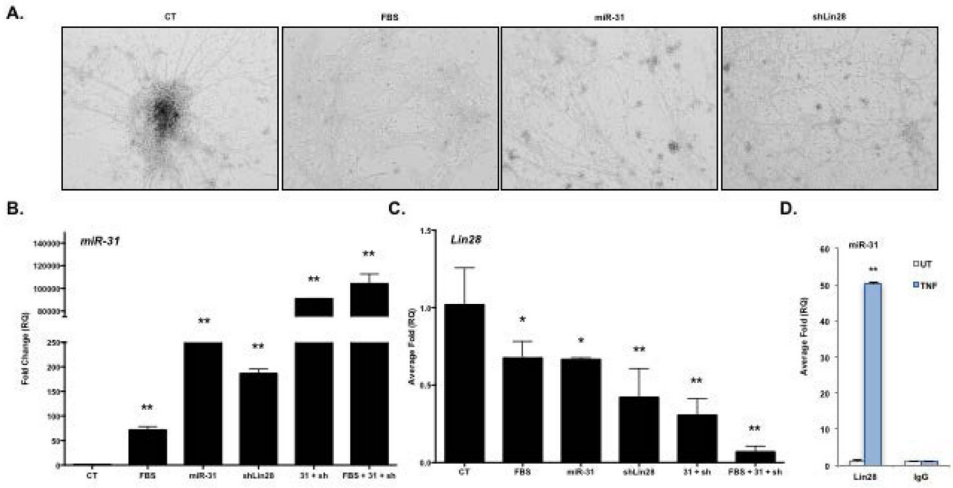

Fig. 7. MiR-31 and/or Loss of Lin28 Promotes Astrocyte Development

A–C. Murine NPCs (E14.5) were transfected with control (CT), miR-31 or shRNA specific for Lin28 (shLin28; sh) and grown in the absence or presence of 10% FBS to induce astrocyte development. **A.** Light microscopy of NPCs grown in presence of CT miR and no FBS (CT), CT miR and FBS (FBS), miR-31 (miR-31) or shLin28 (shLin28) molecules. **B, C.** RNA from cells grown as described above was evaluated by qRT-PCR. (*, $p < 0.05$; **, $p < 0.001$). **D.** U251-MG cells, which express both miR-31 and Lin28, were grown in the absence or presence of TNF (10 ng/ml) for 4 h, and antibodies for Lin28 or IgG were used to immunoprecipitate Lin28 from whole cell lysates. The co-immunoprecipitated RNA was purified and analyzed by qRT-PCR. (**, $p < 0.001$).

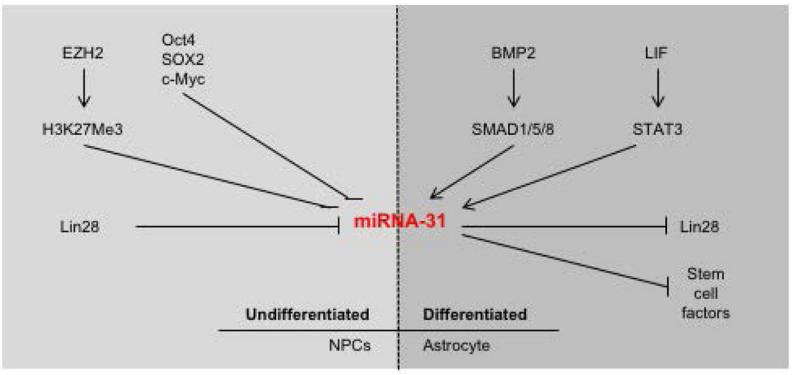

Fig. 8. The Role of MiR-31 During Astrocyte Development

In undifferentiated NPCs (light grey box; left side), miR-31 expression and/or activity is suppressed by Lin28 and other stem cell factors such as Oct4, SOX2 and c-Myc, and PRC2-mediated (EZH2) histone methylation (H3K27Me3). During astrocyte development (dark grey box; right side), BMP2 and LIF signaling through SMAD1/5/8 and STAT3, respectively, induce miR-31 expression. Once induced, miR-31 inhibits Lin28 expression, which coincides with reduced levels of other stem cell factors. We propose the balance between Lin28 and miR-31 expression helps decide the fate of NPCs undergoing astrocyte differentiation.